ELASTIC BEHAVIOUR UNDER COMPRESSIVE STRESSES STATES OF SINTERED METALLIC PARTS

M. D. Riera, I. Marbá and J. M. Prado

Universidad Politécnica de Cataluña. Centre Tecnològic de Manresa.
Avda. Bases de Manresa, 1
08040- MANRESA (Barcelona). Spain

Abstract

The mechanical response in service of a component is mainly determined by its elastic behaviour. Traditionally, metallic materials have been characterized by means of tensile tests, even in the case of sintered ones. In this condition, the elasticity of sintered parts has been always supposed to be linear, with a Young modulus dependent on the density. However, no attention has received the elastic behaviour under compressive stresses.

In this work, the authors present the results obtained from cyclic uniaxial compression tests applied on sintered metallic samples with different densities. The elastic behaviour under compression is no longer linear and different mechanisms occur during the deformation process. Assuming a power law relating compressive stress and strain, an elastic modulus dependent on the density and the loading path has been obtained.

Introduction

Elastic properties determine the mechanical behaviour of structural components, in spite of that the elastic behaviour of porous sintered materials are worst known and understood than when they are fully dense. However, it is well known that porosity markedly reduces the elastic modulus, and that the decrease is roughly proportional to porosity content up to values between 15 and 20%. The Young´s modulus has been measured in tension for a wide range of materials made from metal and ceramic powders [1,2,3]. Nevertheless, very few data are available for the elastic modulus in compression probably because it is assumed that its behaviour should be similar to that of tension. However, the mechanical response of porous materials to tensile or compressive loading can be very different. Tensile loads are supported by the welded necks among particles, but under compressive loads pore closing can take place increasing the practical load bearing area. Therefore, the tensile and compressive elastic behaviour of porous materials can be appreciably different.

The object of the present work has been to study the elastic behaviour of porous steels under compressive stresses, taken also into account the effect of the amount of porosity present in the specimens.

Experimental technique

The metal powder used in this work was the *DISTALOY AE*; an alloyed iron-based atomised powder manufactured by Höganäs with the chemical composition shown in Table 1.

Table 1.- Chemical composition of the *DISTALOY AE*.

Nickel	Copper	Molybdenum	Iron
4%	1.5%	0.5%	94%

The compacted material contained a 98.5% of the type of powder above defined, 1% of Acrawax as a lubricant and 0.5% of graphite in order to obtain the adequate strength after sintering.

Samples were of cylindrical shape with a diameter of 10 mm and a height of 15 mm; they were die compacted to five different densities: 5.42, 5.96, 6.69, 6.92 and 7.08 Mg/m^3 and sintered at 1050ºC during 30 minutes.

Cyclic uniaxial compression tests were done using an Instron 5585 universal tests equipment. Axial strain, $\varepsilon_{ax,}$ was measured by monitoring the displacement of the movable crosshead of the testing machine, whereas for the radial strain, ε_r, a diametrical extensometer was used. The volumetric strain, $\varepsilon_{v,}$ has been calculated by means of using the following expression:

$$\varepsilon_{ax} + 2\,\varepsilon_r = \varepsilon_v \qquad (1)$$

During the cycling the axial load is increased by a fixed amount in each cycle; in this way the unloading part of a cycle can be considered as elastic; however in the following reloading the sample will behave elastically only up to the load level reached in the previous cycle.

Experimental results and discussion

The type of curves obtained when the applied axial true stress, σ, is represented as a function of ε_{ax} and ε_v are shown in Figs.1 and 2 for the case of a sample compacted to a density of 6.69 Mg/m^3 .

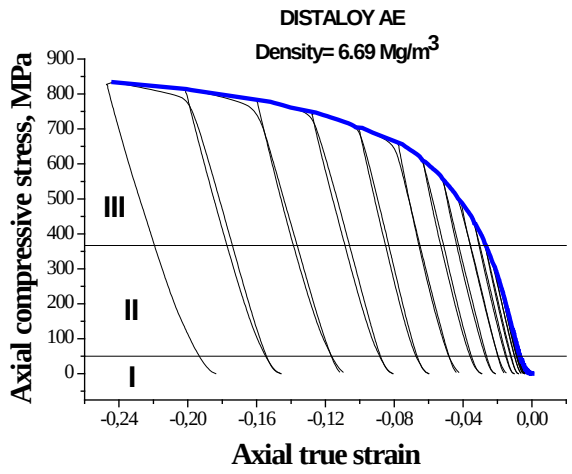

Fig. 1.- Axial true strain during cyclic compression.

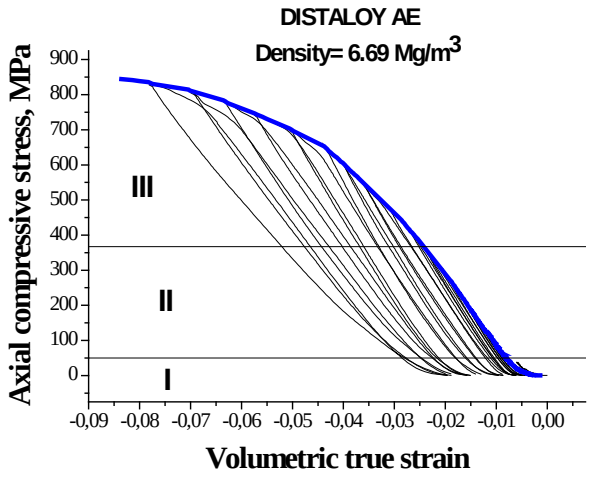

Fig. 2.- Volumetric true strain during cyclic compression.

These plots show the existence of an initial short *foot* (region I) in which plastic densification takes place, followed by a stage of mainly elastic deformation (region II), and a final part of intense plastic strain (region III) of the specimen which leads to its failure by plastic instability. Similar curves were obtained for the other densities under study.

An important feature of the elastic loading-unloading cycles that can be observed in the above figures is the non-linear dependence between the applied true stress and the axial and volumetric true strains. This is even more clearly shown in Figs. 3 to 6 where the elastic part of the loading cycles in Figs. 1 and 2 and their subsequent unloadings are all represented after having been shifted to the origin of coordinates.

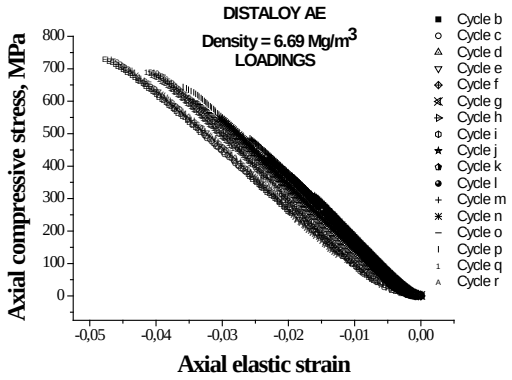

Fig. 3.- Axial strain during the elastic loadings.

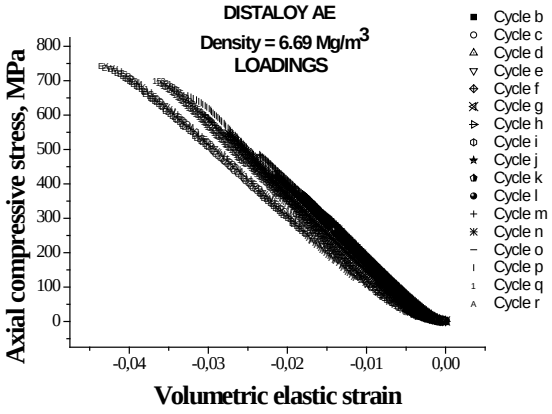

Fig. 4.- Volumetric strain during the elastic loadings.

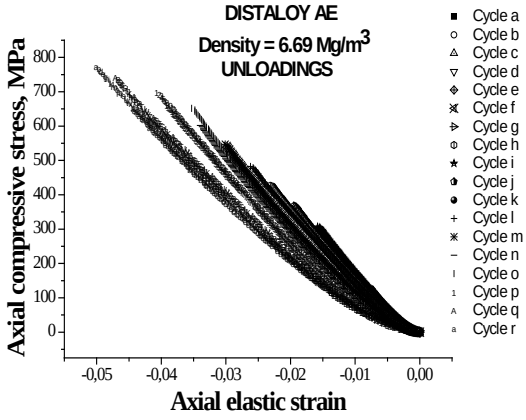

Fig. 5.- Axial strain during the unloadings.

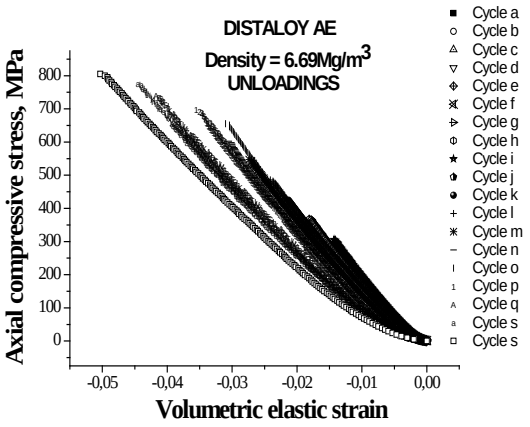

Fig. 6.- Volumetric strain during the unloadings.

The elastic behaviour under compression differs from that observed during the unloading part of the test. Figures 3 to 6 reflect this feature, which can be better analysed when a double logarithmic representation of both axial, ε^{el}_{ax}, and volumetric, ε^{el}_{v}, elastic deformations is used. The following graphs present the results corresponding to the elastic part of the loadings (Figs. 7 and 8) and to the unloadings (Figs. 9 and 10).

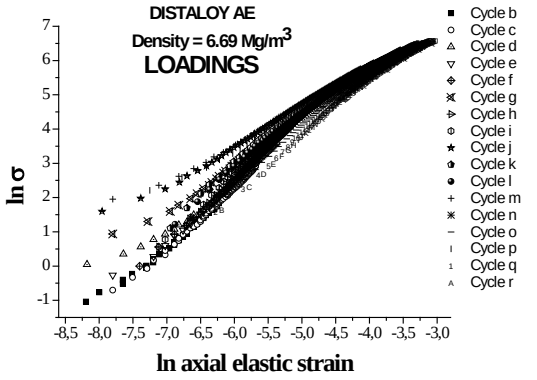

Fig. 7.- Axial strain in the logarithmic space.

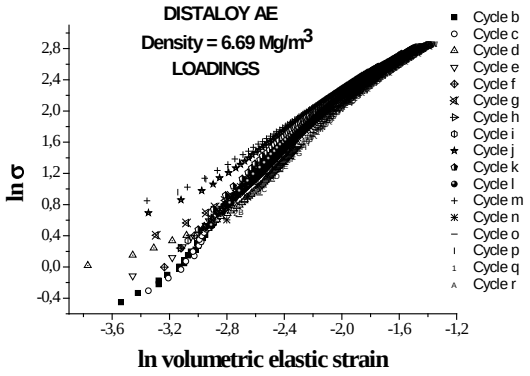

Fig. 8.- Volumetric strain in the logarithmic space.

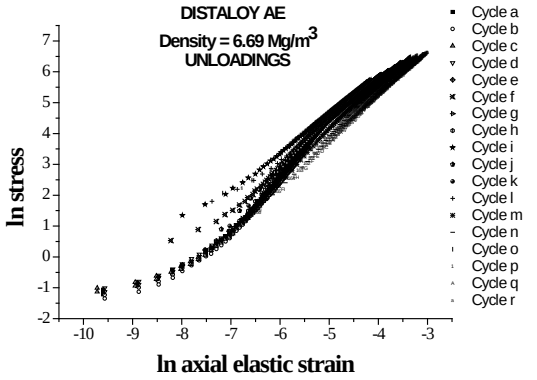

Fig. 9.- Axial strain in the logarithmic space.

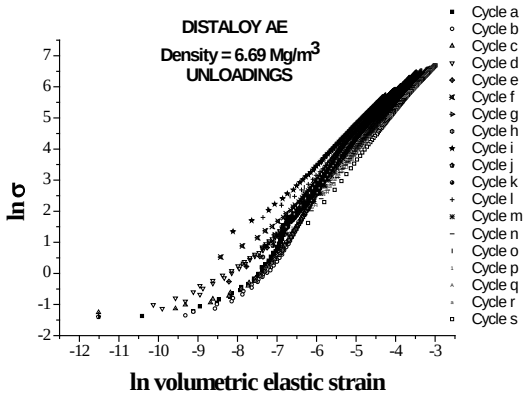

Fig. 10.- Volumetric strain in the logarithmic space.

The relationships between $ln\ \sigma_{ax}$ and $ln\ \varepsilon^{el}_{ax,\,v}$ hold for all the densities studied schemes such as those showed in Figs. 11 and 12 which correspond to the elastic loadings and to the unloadings, respectively.

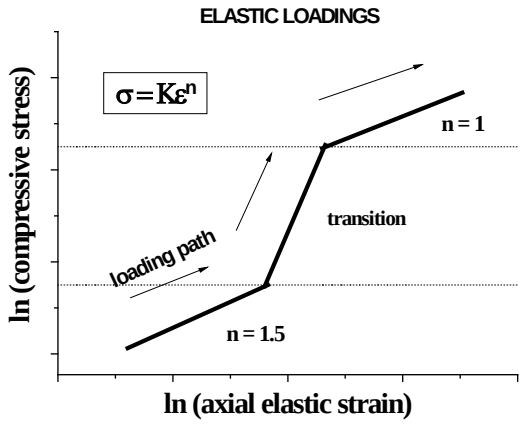

Fig. 11.- Scheme of the evolution of the axial strain in the logarithmic space during the elastic loadings.

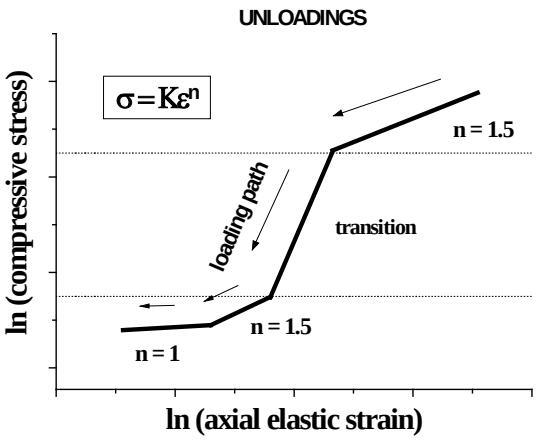

Fig. 12.- Scheme of the evolution of the axial strain in the logarithmic space during the unloadings.

Most of the real sintered metallic compacts can be considered to be interpenetrating networks of metal and void. As the amount of porosity increases the void network increases at the expense of the metal network [2]. According to [4], at low porosity levels the pores are all closed, the first open pores being measured at about 6% of total porosity. At porosity levels greater than 13-14% the pores are almost completely interconnected. The specimens tested for the present work have porosities in the range of 8 to 30%; therefore, their pore structure will be mainly constituted by irregularly distributed, irregularly shaped, interconnected voids; all these features affect the mechanical response of sintered parts.

Schematic curves in Figs 11 and 12 show clear differences in the values of their slopes; this is due to the fact that different mechanisms are governing each stage of the deformation.

During the first stages of the compression test, pore closing dominates the deformation of the material; the contact between the original particles, the necks, increase, and a model of the type of that defined by Hertz [5] would be adequate to describe the elastic behaviour of this material; a power law ($\sigma = K\{\varepsilon^{el}\}^n$) with an exponent, n, of about 1.5 is fulfilled by all the experimental results (Figs. 3, 4 and scheme 11). In the stage of the highest compressive stresses the pores are closed and the linear elasticity of the metallic material is the main mechanism governing the mechanical behaviour; therefore, the part of the curve in Fig. 11, which corresponds to high stresses, has a slope of 1.

The unloading part (Fig. 5, 6 and scheme 12) of the test is characterized by, first of all, a pore opening process. Again, the slope of the logarithmic stress-strain curve is about 1.5, as in the elastic contact between particles occur; after being the pores open, the elastic strain of the metallic skeleton is the phenomenon controlling the deformation of sintered metallic pieces. The slope of the stress-strain relationship in the logarithmic space is in this case equal to 1.

According to the already presented experimental data (Figs. 3 to 10), a power law of the type of:

$$\sigma_{ax} = K\left(\varepsilon_{ax}^{el}\right)^n \qquad (2)$$

describe rather well the elasticity of the sintered material during its unloading after compression. In this equation, σ_{ax} is the applied compressive true stress; ε^{el}_{ax}, the axial elastic true strain, and K and n are two parameters of the material.

In this case, an elastic modulus, E, can be derived from (2):

$$E = \frac{\partial\sigma}{\partial\varepsilon} = nK^{1/n}\sigma^{\frac{n-1}{n}} \qquad (3)$$

In order to determine the value of E, a yield stress dependent on the density has been defined as the stress with an axial plastic strain of 0.03 (see Fig. 1); the values of K and n have been those measured in this yield state. The results obtained are represented in Fig. 13 as the evolution of the elastic modulus, E, against the applied stress corresponding to different densities.

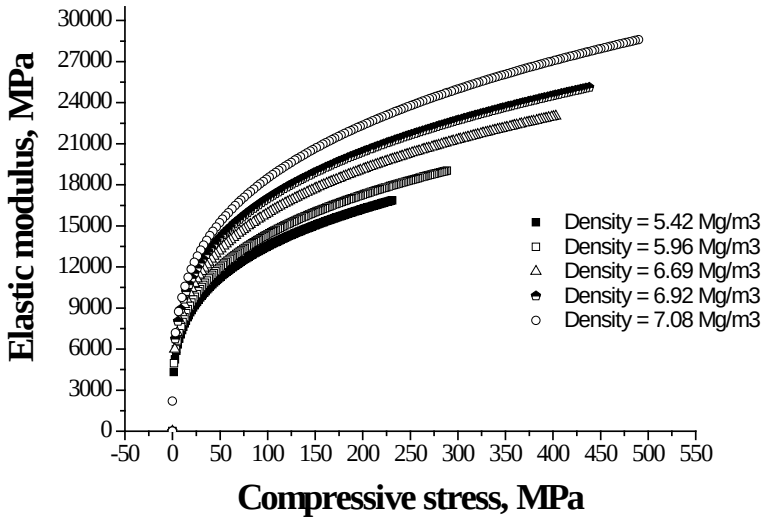

Fig. 13.- Evolution of the elastic modulus in compressive states.

Conclusions

1. The elastic behaviour in compressive states of sintered metallic parts is, in general, non-linear and characterised by different mechanisms of deformation.
2. The amount of porosity and the shape and interconnectivity of pores are responsible for the complex elasticity showed by these materials.
3. Assuming a power law to model the elastic strain of sintered metallic compacts, an elastic modulus dependent on the density and the loading path can be obtained.
4. Further research is needed to reach a better understanding of the mechanical behaviour under compressive stresses of powder sintered materials.

References

[1] *Metals Handbook. 9th ed.* Vol. 7. American Society for Metals. Metals Park. OH. 1984.

[2] R. Haynes and J. T. Egediege. *Effect of porosity and sintering conditions on elastic constants of sintered irons*. Powder Metallurgy. Vol. 32, No. 1. 1989.

[3] J. R. Moon. *Elastic moduli of powder metallurgy steels*. Powder Metallurgy. Vol. 32, No. 2. 1989.

[4] H. H. Hausner, K. H. Mal. *Handbook of Powder Metallurgy. 3rd. ed.* Chemical Publishing Inc. New York. 1989.

[5] S. Timoshenko and J. N. Goudier. *Theory of Elasticity*. Second edition. Ed. McGraw-Hill. New York, 1951.